

Microsolvation of sodium acetate in water: Anion photoelectron spectroscopy and *ab initio* calculations

Wen-Jing Zhang, Gao-Lei Hou, Peng Wang, Hong-Guang Xu, Gang Feng, Xi-Ling Xu, and Wei-Jun Zheng^{a)}

Beijing National Laboratory for Molecular Sciences, State Key Laboratory of Molecular Reaction Dynamics, Institute of Chemistry, Chinese Academy of Sciences, Beijing 100190, China

(Received 4 May 2015; accepted 20 July 2015; published online 4 August 2015)

To understand the microsolvation of sodium acetate (CH_3COONa , NaOAc) in water, we studied $\text{NaOAc}(\text{H}_2\text{O})_n^-$ ($n = 0-3$) clusters by photoelectron spectroscopy. We also investigated the structures of $\text{NaOAc}(\text{H}_2\text{O})_n^-$ ($n = 0-5$) anions and $\text{NaOAc}(\text{H}_2\text{O})_n$ ($n = 0-7$) neutrals by quantum chemistry calculations. By comparing the theoretical results with the photoelectron experiment, the most probable structures of $\text{NaOAc}(\text{H}_2\text{O})_n^{-/0}$ ($n = 0-3$) were determined. The study also shows that, with increasing n , the solvent-separated ion pair (SSIP) structures of $\text{NaOAc}(\text{H}_2\text{O})_n^-$ anions become nearly energetically degenerate with the contact ion pair (CIP) structures at $n = 5$, while the SSIP structures of the neutral $\text{NaOAc}(\text{H}_2\text{O})_n$ clusters appear at $n = 6$ and become dominant at $n = 7$. © 2015 AIP Publishing LLC. [<http://dx.doi.org/10.1063/1.4927668>]

I. INTRODUCTION

The dissolution of salts is a fundamental process in chemistry. Dissolved salts play important roles in chemical reactions,^{1,2} biochemistry,^{3,4} marine chemistry,⁵ atmospheric chemistry,⁶ and our daily life.⁷ Therefore, many theoretical⁸⁻¹⁹ and experimental²⁰⁻²⁹ studies have investigated the microscopic mechanisms of salt dissolution. Special attention has been paid to investigate the transition between salt contact ion pairs (CIPs) and solvent-separated ion pairs (SSIPs) in water,^{13,30} as well as the correlation of salt effects with the Hofmeister series.^{31,32} Previously, our group has employed anion photoelectron spectroscopy and theoretical calculations to investigate the microsolvation of a number of salts such as NaBO_2 ,³³ LiBO_2 ,³⁴ LiI , CsI ,³⁵ NaCl ,³⁶ and Li_2SO_4 ³⁷ in water.

Sodium acetate (CH_3COONa , NaOAc) is an important salt that is widely used in the industry and our daily life. Acetic acid is not only commonly used in our daily life, but also is one of the most abundant organic compounds in the atmosphere.^{38,39} The hydration of acetic acid has been investigated recently using high-resolution microwave spectroscopy⁴⁰ and matrix-isolated infrared spectroscopy.⁴¹ The hydration of acetate ion has been studied using dielectric relaxation spectroscopy,⁴² photoelectron spectroscopy, and *ab initio* calculations.⁴³ The acetate anion and sodium cation are both considered to be kosmotropes (which can be strongly hydrated) in the anionic and cationic Hofmeister series, respectively.⁴⁴ The solvation process of sodium acetate might differ substantially from the behavior of simple diatomic salts (such as alkali halides)³⁵ as both the hydrophilic and hydrophobic interactions are involved because of the presence a hydrophilic group ($-\text{COO}^-$) and a hydrophobic group ($-\text{CH}_3$) in the acetate anion.

In addition, sodium acetate can be used as a simple model for interrogating the interactions between cations and protein

surfaces because some proteins have carboxylate groups to which alkali cations can bind.⁴⁵ The aqueous solvation of sodium acetate may mimic the interactions between alkali cations and protein surfaces in water, and, in this manner, can provide valuable information about the salting in and salting out of proteins in salt water solutions. Interactions between alkali cations and carboxylates have been studied in solutions and at interfaces using a variety of techniques such as X-ray absorption spectroscopy,^{46,47} femtosecond mid-IR pump-probe spectroscopy,⁴⁸ and Raman spectroscopy,⁴⁹ as well as theoretical modeling.⁵⁰⁻⁵²

In this work, to advance our understanding of the solvation behavior of sodium acetate, we investigated $\text{NaOAc}(\text{H}_2\text{O})_n^-$ clusters using mass-selected anion photoelectron spectroscopy and *ab initio* calculations.

II. EXPERIMENTAL AND COMPUTATIONAL METHODS

A. Experimental method

The experiments were conducted with a home-built apparatus consisting of a time-of-flight mass spectrometer and a magnetic-bottle photoelectron spectrometer, which has been described elsewhere.⁵³ Briefly, the $\text{NaOAc}(\text{H}_2\text{O})_n^-$ cluster anions were produced in a laser vaporization source by ablating a rotating and translating sodium acetate solid disc target with the second harmonic (532 nm) light pulses of a Nd:YAG laser, while helium carrier gas at a 4 atm backing pressure seeded with water vapor was allowed to expand through a pulsed valve to generate hydrated NaOAc^- and to cool the formed clusters. The cluster anions were mass-analyzed by the time-of-flight mass spectrometer. The $\text{NaOAc}(\text{H}_2\text{O})_n^-$ ($n = 0-3$) clusters were each mass-selected and decelerated before being photodetached by another Nd:YAG laser. The electrons resulting from photodetachment were energy-analyzed by the magnetic-bottle photoelectron spectrometer. The photoelectron spectra were calibrated using the spectra of Bi^- and Cs^- taken at similar

^{a)} Author to whom correspondence should be addressed. Electronic mail: zhengwj@iccas.ac.cn

conditions. The instrumental resolution was approximately 40 meV for electrons with 1 eV kinetic energy.

B. Computational method

The Gaussian09⁵⁴ program package was used for all calculations. The structures of $\text{NaOAc}(\text{H}_2\text{O})_n^-$ ($n = 0-5$) anions and neutral $\text{NaOAc}(\text{H}_2\text{O})_n$ ($n = 0-7$) were optimized with density functional theory (DFT) employing the long-range corrected hybrid functional LC- ω PBE.⁵⁵⁻⁵⁸ The standard Pople type 6-311++G(d, p) basis set was used for all the atoms. The initial structures of $\text{NaOAc}(\text{H}_2\text{O})^-$ were obtained by varying the positions of the water molecules and those of the larger clusters were generated from the smaller ones by adding water molecules to different positions. Harmonic vibrational frequencies were calculated to confirm that the optimized structures correspond to real local minima. In order to obtain more accurate energies, the single point energies of the small $\text{NaOAc}(\text{H}_2\text{O})_n^-$ cluster anions with $n \leq 3$, and their corresponding neutral species, were also calculated using coupled-cluster theory including single, double, and non-iterative triple excitations (CCSD(T))⁵⁹ and with aug-cc-pVDZ basis set based on the structures optimized at the LC- ω PBE/6-311++G(d, p) level. The vertical electron detachment energies (VDEs) of the $\text{NaOAc}(\text{H}_2\text{O})_n^-$ ($n = 0-3$) anions were calculated as the energy differences between the electronic ground states of the neutrals and anions, with the energies of the neutrals computed at the geometries of their corresponding anionic species. The theoretical adiabatic electron detachment energies (ADEs) were calculated as the energy differences between the neutrals and the anions, with the energies of the neutrals computed after allowing relaxation to the nearest

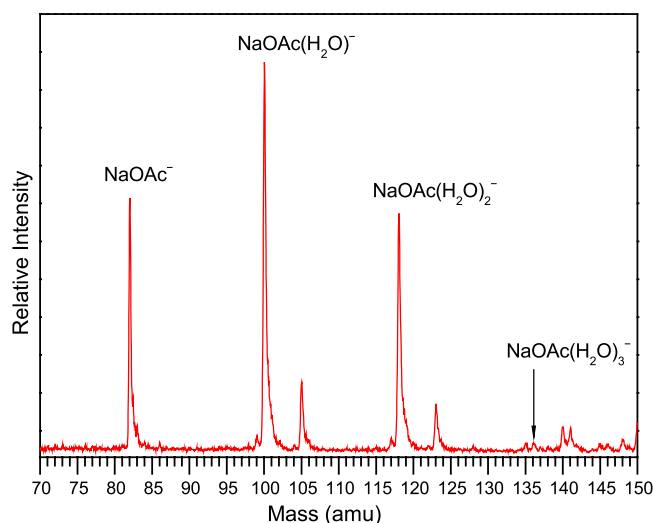


FIG. 1. Mass spectrum of $\text{NaOAc}(\text{H}_2\text{O})_n^-$ ($n = 0-3$) cluster anions.

local minima from the starting geometries of the corresponding anions. The relative energies between different isomers were corrected by the zero-point vibrational energies obtained at the LC- ω PBE/6-311++G(d, p) level.

III. EXPERIMENTAL RESULTS

Figure 1 shows a typical mass spectrum of cluster anions generated in the experiments. The mass peaks of the $\text{NaOAc}(\text{H}_2\text{O})_n^-$ ($n = 0-3$) series are observed although the $\text{NaOAc}(\text{H}_2\text{O})_3^-$ peak is very weak. The photoelectron spectra of $\text{NaOAc}(\text{H}_2\text{O})_n^-$ ($n = 0-3$) recorded with 1064 and 532 nm are presented in Figure 2. The VDEs and ADEs of the

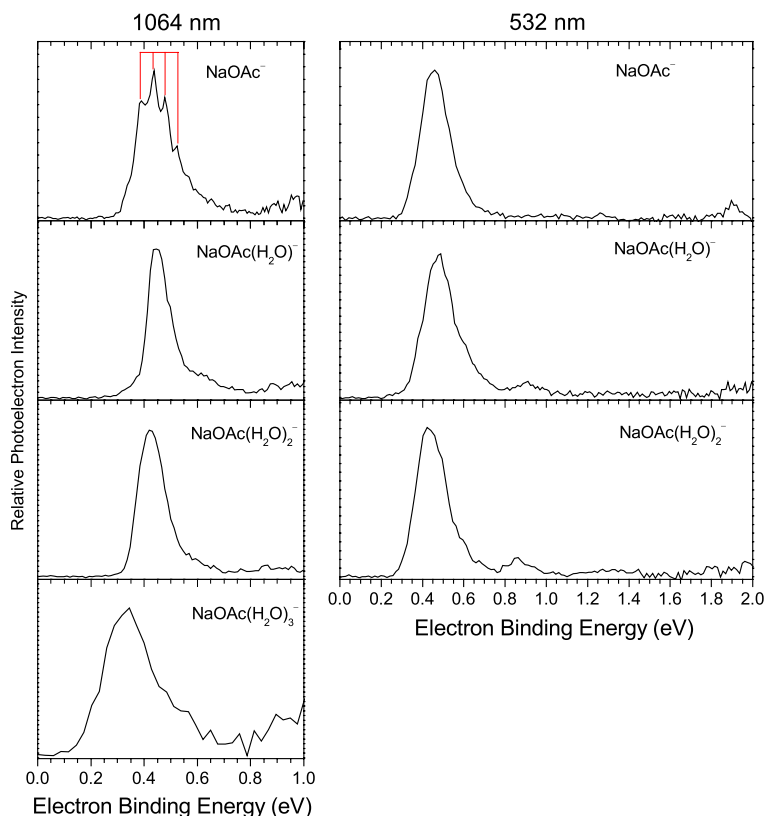


FIG. 2. Photoelectron spectra of $\text{NaOAc}(\text{H}_2\text{O})_n^-$ ($n = 0-3$) clusters recorded with 1064 and 532 nm photons.

TABLE I. Experimentally observed VDEs and ADEs of $\text{NaOAc}(\text{H}_2\text{O})_n^-$ ($n = 0-3$) from their photoelectron spectra.

Cluster	ADE (eV)	VDE (eV)
NaOAc^-	0.39 ± 0.03	0.44 ± 0.03
$\text{NaOAc}(\text{H}_2\text{O})^-$	0.42 ± 0.08	0.45 ± 0.08
$\text{NaOAc}(\text{H}_2\text{O})_2^-$	0.38 ± 0.08	0.42 ± 0.08
$\text{NaOAc}(\text{H}_2\text{O})_3^-$	0.20 ± 0.08	0.34 ± 0.08

$\text{NaOAc}(\text{H}_2\text{O})_n^-$ ($n = 0-3$) clusters as estimated from the photoelectron spectra are summarized in Table I. To account for peak broadening due to instrumental resolution, the ADE of each cluster was evaluated by adding the instrumental resolution to the onset of the first peak in the spectrum. The onset of the first peak was determined by drawing a straight line along the leading edge of that peak across the spectrum baseline.

In Figure 2, we can see that the photoelectron spectrum of NaOAc^- recorded with 532 nm photons has a broad feature centered at 0.44 eV, which can be resolved into four peaks centered at 0.39, 0.44, 0.48, and 0.52 eV in the 1064 nm spectrum. The first peak at 0.39 eV designates the ADE, and the others correspond to the vibrational progression (Na–O stretch) of the NaOAc neutral. The vibrational frequency of Na–OAc is estimated to be $350 \pm 50 \text{ cm}^{-1}$ on the basis of the spaces between those peaks (see supplementary material).⁶⁰ The VDE of NaOAc^- is estimated to be $0.44 \pm 0.03 \text{ eV}$ based on the spectrum at 1064 nm. The peak at 0.39 eV corresponds to the transition from the vibrational ground state of NaOAc^- to that of the NaOAc neutral; thus, the electron affinity of NaOAc is determined to be $0.39 \pm 0.03 \text{ eV}$.

The 1064 nm spectrum of $\text{NaOAc}(\text{H}_2\text{O})^-$ shows a major feature centered at 0.45 eV. In addition to the same major feature observed at 1064 nm, the 532 nm spectrum has a small feature centered at 0.91 eV. The small peak at 0.91 eV is not observed in the NaOAc^- spectrum. It is likely attributable to the water O–H stretch because it is higher than the first feature by $\sim 0.46 \text{ eV}$ ($3710 \pm 200 \text{ cm}^{-1}$), which is close to the O–H stretching frequency of the water molecule.

The 532 nm spectrum of $\text{NaOAc}(\text{H}_2\text{O})_2^-$ has a broad feature centered at 0.42 eV and a small one centered at 0.86 eV. Similar to the case of $\text{NaOAc}(\text{H}_2\text{O})^-$, the $\text{NaOAc}(\text{H}_2\text{O})_2^-$ photoelectron peak at 0.86 eV is higher than the first peak by $\sim 0.44 \text{ eV}$ ($3550 \pm 200 \text{ cm}^{-1}$), close to the O–H stretching frequency of the water molecule. Note that the second peaks of $\text{NaOAc}(\text{H}_2\text{O})^-$ and $\text{NaOAc}(\text{H}_2\text{O})_2^-$ are less obvious at 1064 nm; this is probably because of the lower detachment cross-sections of these peaks at 1064 nm or the lower detection-efficiency of the low-kinetic-energy electrons. The 1064 nm spectrum of $\text{NaOAc}(\text{H}_2\text{O})_3^-$ has a broad peak centered at 0.34 eV. The 532 nm spectrum of $\text{NaOAc}(\text{H}_2\text{O})_3^-$ has a very low signal-to-noise ratio due to the low ion intensity, thus, it is not shown here.

IV. THEORETICAL RESULTS

We optimized the structures of $\text{NaOAc}(\text{H}_2\text{O})_n^-$ ($n = 0-5$) anions and neutral $\text{NaOAc}(\text{H}_2\text{O})_n$ ($n = 0-7$) at the LC- ω PBE/6-311++G(d, p) level. As we will show later, the calculated structures indicate that the SSIP and CIP structures of the

anions are almost degenerate in energy at $n = 5$ while the CIP structures of the neutrals are dominant at $n \leq 5$. At $n = 7$, the SSIP structures of neutral $\text{NaOAc}(\text{H}_2\text{O})_n$ become more stable than the CIP structures. Next, we present the results of theoretical calculations as well as the comparison between the theory and experiment in detail.

A. $\text{NaOAc}(\text{H}_2\text{O})_n^-$ and $\text{NaOAc}(\text{H}_2\text{O})_n$ ($n = 0-3$)

The optimized geometries of the low-lying isomers of $\text{NaOAc}(\text{H}_2\text{O})_n^-$ ($n = 0-3$) clusters and those of their neutral counterparts are presented in Figures 3 and 4, respectively, with the most stable structures on the left. The calculated VDEs and ADEs of the $\text{NaOAc}(\text{H}_2\text{O})_n^-$ ($n = 0-3$) clusters are listed in Table II along with their experimental VDEs and ADEs. It can be seen from Table II that the results of both LC- ω PBE and CCSD(T) methods are in good agreement with the experimental values. In the following discussion of small $\text{NaOAc}(\text{H}_2\text{O})_n^-$ cluster anions with $n \leq 3$ and their neutral counterparts, we will mainly refer to the CCSD(T) results.

1. NaOAc^- and NaOAc

The most stable structure of NaOAc^- is a bidentate structure with the Na atom binding to both O atoms of the acetate anion, which is consistent with the previous study.^{47,52} Both Na–O bond lengths in NaOAc^- are calculated to be 2.32 Å. The theoretical VDE of isomer 0A calculated by the CCSD(T) method is about 0.40 eV, in good agreement with the experimental VDE of 0.44 eV.

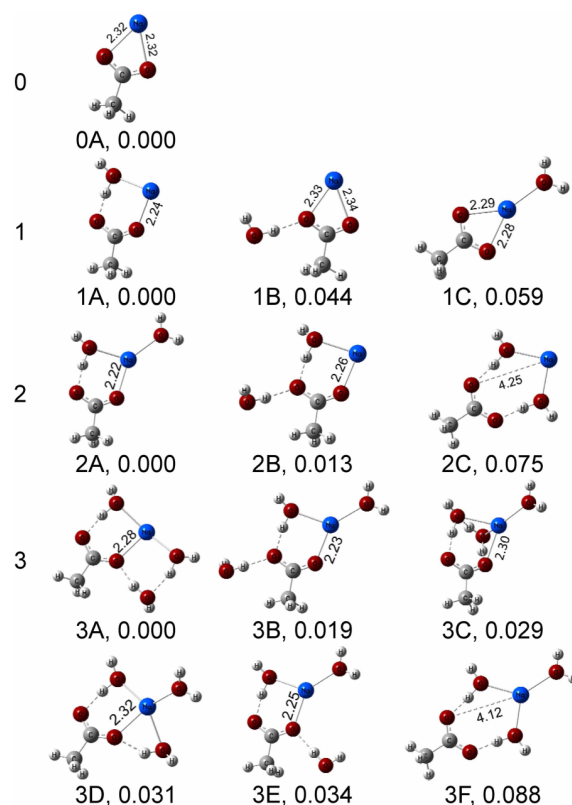


FIG. 3. Typical low-lying isomers of $\text{NaOAc}(\text{H}_2\text{O})_n^-$ ($n = 0-3$). The relative energies are shown in eV. The relative energies were obtained at the CCSD(T)/aug-cc-pVDZ//LC- ω PBE/6-311++G(d, p) level of theory.

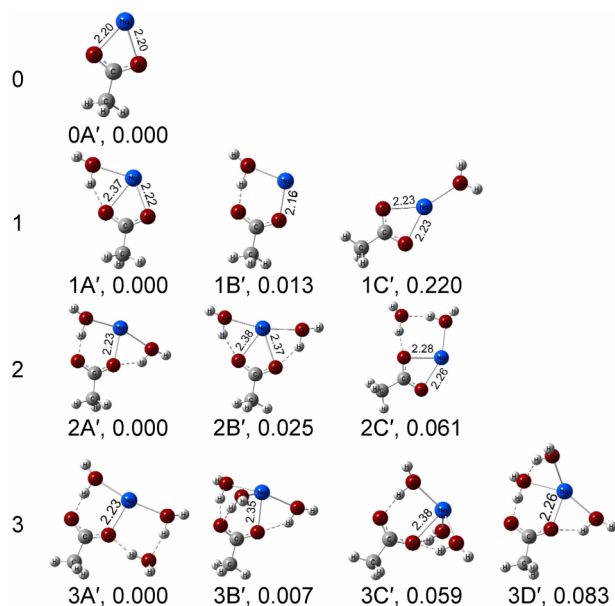


FIG. 4. Typical low-lying isomers of neutral $\text{NaOAc}(\text{H}_2\text{O})_n$ ($n = 0-3$) clusters. The relative energies are shown in eV. The relative energies for $n = 0-3$ were obtained at the CCSD(T)/aug-cc-pVDZ//LC- ω PBE/6-311++G(d,p) level of theory.

Our calculations show that the ground state geometry of neutral NaOAc is also a bidentate structure with slightly shorter Na–O distances than those in the anion. The frequency of the Na–OAc stretch in neutral NaOAc is calculated to be 338 cm^{-1} , in agreement with the experimental value of 350 cm^{-1} measured in this work. Natural bond orbital (NBO) charge analysis of neutral NaOAc predicts the charge on the Na atom as $+0.929\text{ e}$, with that on the acetate group as -0.929 e . When an excess electron is added to NaOAc to form the anion, the excess electron mainly localizes on the Na atom, the

positive pole of the molecule (see supplementary material),⁶⁰ and hence reduces the Coulombic attraction between the $\text{Na}^+ - \text{OAc}^-$ ion pair, which may explain why the Na–O distances in the NaOAc^- anion are longer than those in the neutral NaOAc.

2. $\text{NaOAc}(\text{H}_2\text{O})^-$ and $\text{NaOAc}(\text{H}_2\text{O})$

The lowest energy geometry of $\text{NaOAc}(\text{H}_2\text{O})^-$ (isomer 1A) has a six-membered ring structure with a water molecule inserted between one of the Na–O bonds of the sodium acetate. The water molecule interacts with the sodium atom through its O atom and with an acetate oxygen atom through hydrogen bond formation. The six-membered ring structure is similar to the case of $\text{AcOH}-(\text{H}_2\text{O})$ complex.^{40,41} The theoretical VDE of isomer 1A (0.35 eV) is in reasonable agreement with the experimental VDE (0.45 eV). Isomer 1B has a bidentate structure with one H atom of the water molecule interacting with one O atom of the acetate through a hydrogen bond. It is less stable than isomer 1A by 0.044 eV . Its VDE is calculated to be 0.58 eV . Isomer 1C also has a bidentate structure but with the water molecule connecting to the Na atom via its O atom. It is higher in energy than isomer 1A by 0.059 eV although its VDE (0.44 eV) is close to the experimental value. That implies that isomer 1A is the dominant experimental species.

The ground state geometry of neutral $\text{NaOAc}(\text{H}_2\text{O})$ ($1\text{A}'$) has a bidentate structure with one O–H bond of the water molecule approaching one of the Na–O bonds of acetate. No Na–O bond in isomer $1\text{A}'$ is broken, which is different from the case of the anion. The second isomer of neutral $\text{NaOAc}(\text{H}_2\text{O})$ ($1\text{B}'$) is similar to the most stable structure of the $\text{NaOAc}(\text{H}_2\text{O})^-$ anion. It is higher in energy than isomer $1\text{A}'$ by only 0.013 eV . Isomer $1\text{C}'$ is similar to isomer 1C with the water molecule connecting to the Na atom via its O atom.

TABLE II. Relative energies of the low energy isomers of $\text{NaOAc}(\text{H}_2\text{O})_n^-$ ($n = 0-3$) and comparison of their theoretical VDEs and ADEs to the experimental values. The calculations were performed at the CCSD(T)/aug-cc-pVDZ//LC- ω PBE/6-311++G (d,p) level of theory. The isomers set in bold are the probable ones detected in the experiment.

Isomer	ΔE (eV)	ADE (eV) ^a				VDE (eV)		
		Theoretical				Theoretical		
		CCSD(T)	LC- ω PBE	CCSD(T)	Expt.	LC- ω PBE	CCSD(T)	Expt.
NaOAc^-	0A	0.000	0.48	0.39	0.39	0.53	0.40	0.44
$\text{NaOAc}(\text{H}_2\text{O})^-$	1A	0.000	0.34	0.30	0.42	0.44	0.35	0.45
	1B	0.044	0.25	0.23		0.74	0.58	
	1C	0.059	0.36	0.42		0.39	0.44	
$\text{NaOAc}(\text{H}_2\text{O})_2^-$	2A	0.000	0.12	0.13	0.38	0.34	0.40	0.42
	2B	0.013	0.49	0.44		0.62	0.52	
	2C	0.075	0.09	0.06		0.65	0.56	
$\text{NaOAc}(\text{H}_2\text{O})_3^-$	3A	0.000	0.03	0.04	0.20	0.15	0.10	0.34
	3B	0.019	0.23	0.22		0.45	0.50	
	3C	0.029	0.04	0.04		0.33	0.38	
	3D	0.031	−0.07	−0.05		0.25	0.30	
	3E	0.034	−0.13	−0.08		0.46	0.50	
	3F	0.088	0.39	0.47		0.47	0.53	

^aHere, the experimental ADEs may not represent the real ADEs because of possible significant structural changes between the anions and neutrals. Thus, the experimental ADEs are not used to verify the theoretical calculations.

3. $\text{NaOAc}(\text{H}_2\text{O})_2^-$ and $\text{NaOAc}(\text{H}_2\text{O})_2$

The most stable isomer of $\text{NaOAc}(\text{H}_2\text{O})_2^-$ (2A) has a six-membered ring structure with the first water molecule inserted between one Na–O bond of NaOAc. The second water molecule attaches to the Na atom of NaOAc. The calculated VDE of isomer 2A is about 0.40 eV, in agreement with the experimental value (0.42 eV). Similar to the case of isomer 2A, isomer 2B also has a six-membered ring structure but with the second water molecule forming a hydrogen bond with one O atom of acetate. It is higher in energy than isomer 2A by only 0.013 eV. The calculated VDE of isomer 2B is about 0.52 eV. In isomer 2C one water molecule inserts into each of the two Na–O bonds of sodium acetate, resulting in an eight-membered ring structure. The Na–OAc distance in isomer 2C increases significantly to 4.25 Å because of the introduction of two water molecules between the Na atom and OAc group. Isomer 2C is higher in energy than isomer 2A by 0.075 eV. The VDE of isomer 2C is calculated to be 0.56 eV. Based on the above analysis, we suggest that the major peak in the experimental photoelectron spectrum of $\text{NaOAc}(\text{H}_2\text{O})_2^-$ results from contributions of both isomers 2A and 2B because they are almost degenerate in energy and their VDEs are in agreement with the experimental value.

The most stable structure of neutral $\text{NaOAc}(\text{H}_2\text{O})_2$ (2A') is different from isomer 2A. It has an O–H bond of the second water molecule interacting with the remaining Na–O bond of sodium acetate to form a four-membered ring. Isomer 2B' is less stable than isomer 2A' by only 0.025 eV. It is a bidentate structure with an O–H bond of each water molecule interacting with one Na–O bond of sodium acetate, respectively. Isomer 2C' also has a bidentate structure except that the two water molecules form a water-water hydrogen bond and stay at one side of the same Na–O bond. It is less stable than isomer 2A' by 0.061 eV.

4. $\text{NaOAc}(\text{H}_2\text{O})_3^-$ and $\text{NaOAc}(\text{H}_2\text{O})_3$

The most stable structure of $\text{NaOAc}(\text{H}_2\text{O})_3^-$ (isomer 3A) has a water molecule inserted between one Na–O bond of the sodium acetate to form a six-membered ring. The other two water molecules interact with each other by forming a hydrogen bond and bridge the Na–O bond to form another six-membered ring. Isomer 3B is derived from isomer 2A by attaching the third H_2O to form a hydrogen bond with

an O atom of the acetate. It is less stable than isomer 3A by only 0.019 eV. Isomers 3C, 3D, and 3E are almost degenerate in energy and higher than isomer 3A by 0.029, 0.031, and 0.034 eV, respectively. They are derived from the six-membered ring structure (isomer 1A) by attaching the second and third water molecules to different positions. Isomer 3F is higher in energy than isomer 3A by 0.088 eV and can be considered as evolved from isomer 2C of $\text{NaOAc}(\text{H}_2\text{O})_2^-$ by adding the third H_2O to the Na atom. The Na–OAc distance in isomer 3F is about 4.12 Å. The calculated VDEs of isomers 3A–3F are 0.10, 0.50, 0.38, 0.30, 0.50, and 0.53 eV, respectively. In the experimental spectrum of $\text{NaOAc}(\text{H}_2\text{O})_3^-$, the photoelectron peak centered at 0.34 eV is very broad and spreads from 0.2 to 0.6 eV, indicating that a few isomers may coexist in the experiment. Here, we suggest that isomers 3A–3E coexist in the experiment because they are very close in energy and their VDEs are consistent with the experimental photoelectron spectrum.

For neutral $\text{NaOAc}(\text{H}_2\text{O})_3$, the ground state structure (3A') is similar to the most stable structure of the anion (3A), with slightly shorter Na–O bond. Isomer 3B' is higher in energy than isomer 3A' by only 0.007 eV. It has two water molecules inserted between the same Na–O bond of the NaOAc to form two six-membered rings and the third water molecule interacts with another Na–O bond of the NaOAc. Isomer 3C' is higher in energy than isomer 3A' by 0.059 eV. It has two water molecules interacting with the same Na–O bond with their O atoms pointing toward the Na atom. Isomer 3D' is less stable than isomer 3A' by 0.083 eV. It can be considered as evolved from isomer 2A' by attaching the third water molecule to the Na–O bond formed between the inserting water molecule and the Na atom of the NaOAc.

B. $\text{NaOAc}(\text{H}_2\text{O})_n^-$ ($n = 4-5$) and $\text{NaOAc}(\text{H}_2\text{O})_n$ ($n = 4-7$)

The good agreement between the theoretical results of the small $\text{NaOAc}(\text{H}_2\text{O})_n^-$ clusters ($n = 0-3$) with the experimental data indicates that the LC- ω PBE functional can predict the structures of the $\text{NaOAc}(\text{H}_2\text{O})_n$ clusters very well. This gives us confidence in the predicted structures of the larger clusters, $\text{NaOAc}(\text{H}_2\text{O})_n^-$ ($n = 4-5$) and $\text{NaOAc}(\text{H}_2\text{O})_n$ ($n = 4-7$), obtained by the LC- ω PBE functional. Here, we examine the low-lying isomers of $\text{NaOAc}(\text{H}_2\text{O})_4^-$ and $\text{NaOAc}(\text{H}_2\text{O})_5^-$ in Figure 5 as well as those of neutral $\text{NaOAc}(\text{H}_2\text{O})_n$ ($n = 4-7$) in Figure 6.

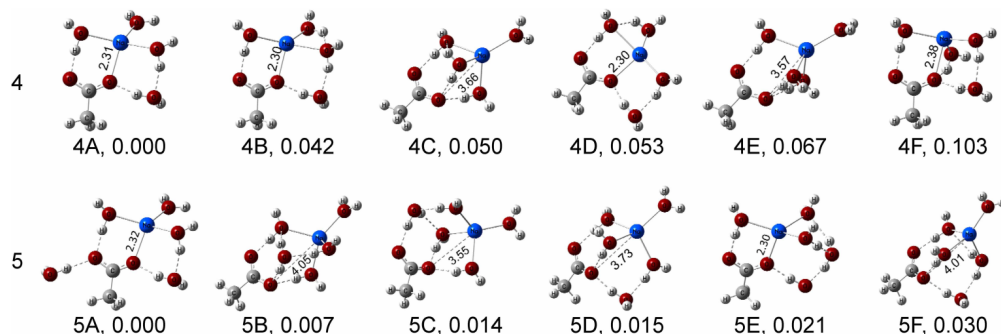


FIG. 5. Typical low-lying isomers of $\text{NaOAc}(\text{H}_2\text{O})_4^-$ and $\text{NaOAc}(\text{H}_2\text{O})_5^-$. The relative energies are shown in eV. The relative energies were obtained at the LC- ω PBE/6-311++G(d, p) level of theory.

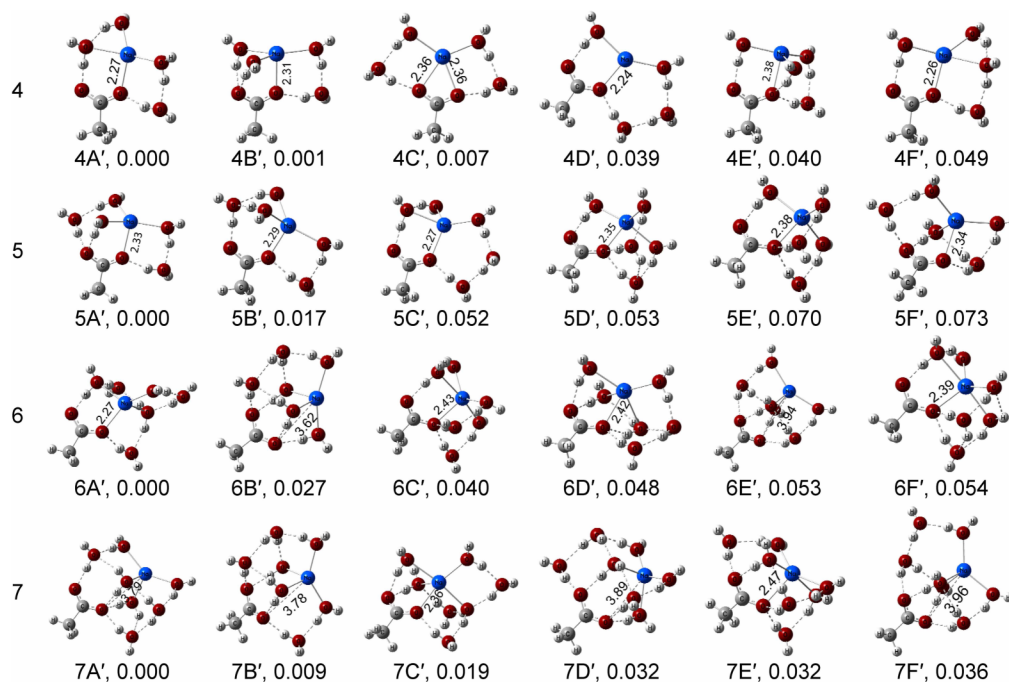


FIG. 6. Typical low-lying isomers of neutral $\text{NaOAc}(\text{H}_2\text{O})_n$ ($n = 4-7$) clusters. The relative energies are shown in eV. The relative energies were obtained at the LC- ω PBE/6-311++G(d, p) level of theory.

1. $\text{NaOAc}(\text{H}_2\text{O})_n^-$ ($n = 4-5$)

Isomers 4A, 4B, 4D, and 4F of $\text{NaOAc}(\text{H}_2\text{O})_4^-$ anion can be considered to be formed from isomer 3A by adding the fourth H_2O to different positions. Isomers 4C and 4E are SSIP structures with Na–OAc distances of 3.66 and 3.57 Å, respectively. For isomers 4C or 4E, the Na atom is surrounded by four water molecules with three of the water molecules inserted between the Na atom and OAc group while the other water molecule remains on the other side of the Na atom. Isomers 4C and 4E are higher in energy than the most stable isomer of $\text{NaOAc}(\text{H}_2\text{O})_4^-$ by 0.050 and 0.067 eV, respectively. For $\text{NaOAc}(\text{H}_2\text{O})_5^-$, the SSIP structures are almost degenerate in energy with the CIP structures. Isomers 5A and 5E of $\text{NaOAc}(\text{H}_2\text{O})_5^-$ anion are CIP structures derived from isomer 4A by attaching the fifth water molecule to different positions. Isomers 5B, 5C, 5D, and 5F are SSIP structures with four water molecules inserted between the Na atom and OAc group and one water molecule on the other side of the Na atom. The Na–OAc distances of 5B, 5C, 5D, and 5F range from 3.55 to 4.05 Å. The energy of the lowest SSIP structure (5B) is higher than the most stable CIP structure by only 0.007 eV.

2. $\text{NaOAc}(\text{H}_2\text{O})_n$ ($n = 4-7$)

The low-lying isomers of neutral $\text{NaOAc}(\text{H}_2\text{O})_4$ are all CIP structures with Na–OAc distances between 2.24 and 2.38 Å. Isomers 4A', 4B', 4E', and 4F' are formed from isomer 3A' by adding the fourth water molecule. Isomer 4C' is a bidentate structure with two water molecules interacting with one Na–O bond and the other two water molecules interacting with the second Na–O bond. Isomer 4D' has a water molecule inserted between the first Na–O bond of the NaOAc to form a six-membered ring, and the other three water molecules

forming a chain and interacting with the second Na–O bond of the NaOAc to form an eight-membered ring. The low-lying isomers of neutral $\text{NaOAc}(\text{H}_2\text{O})_5$ are also CIP structures derived from those of neutral $\text{NaOAc}(\text{H}_2\text{O})_4$. Starting at $n = 6$, the SSIP structures of neutral $\text{NaOAc}(\text{H}_2\text{O})_n$ clusters begin to appear, with isomers 6B' and 6E' displaying SSIP structures and higher in energy than the most stable CIP isomer by 0.027 and 0.053 eV, respectively. For $\text{NaOAc}(\text{H}_2\text{O})_7$, the SSIP structures become more stable than the CIP structures. Isomers 7A', 7B', 7D', and 7F' are all SSIP structures while the CIP structures (7C' and 7E') are higher than the most stable SSIP structure (7A') by 0.019 and 0.032 eV, respectively.

V. DISCUSSION

Both our theoretical calculations and experimental measurements show that the VDE of the most stable isomer of $\text{NaOAc}(\text{H}_2\text{O})_3^-$ is relatively lower than those of $\text{NaOAc}(\text{H}_2\text{O})^-$ and $\text{NaOAc}(\text{H}_2\text{O})_2^-$. That is because the sodium-water interactions are stronger in $\text{NaOAc}(\text{H}_2\text{O})_3$ clusters. The strong Na^+ -water interactions can stabilize the neutral states of $\text{NaOAc}(\text{H}_2\text{O})_n$ clusters, decreasing the energy differences between the neutrals and anions, and therefore reducing the VDEs. The lower VDE of $\text{NaOAc}(\text{H}_2\text{O})_3^-$ indicates that it is more difficult for it to be formed in the experiment. This likely explains why the mass peak of $\text{NaOAc}(\text{H}_2\text{O})_3^-$ is much weaker than those of $\text{NaOAc}(\text{H}_2\text{O})^-$ and $\text{NaOAc}(\text{H}_2\text{O})_2^-$ (Figure 1).

The most stable structures of both NaOAc^- and NaOAc neutral are bidentate structures with the Na atom interacting with both O atoms of acetate anion. Our studies show that the water molecules tend to interact with the hydrophilic part ($-\text{COONa}$) and alienate the hydrophobic part ($-\text{CH}_3$), which is consistent with the decreased surface tension of sodium

acetate solution observed previously.⁵¹ The water molecules prefer to interact with the Na atom via their O atoms and to interact with the O atoms of acetate anions by forming hydrogen bonds. The most stable structures of $\text{NaOAc}(\text{H}_2\text{O})_n^-$ and $\text{NaOAc}(\text{H}_2\text{O})_n$ for $n = 3-5$ are mainly characterized by two types of six-membered rings at the hydrophilic part. The first six-membered ring consists of a Na atom, a $-\text{COO}^-$ group, and an O–H bond of a water molecule. The second six-membered ring is composed of a Na–O bond of NaOAc and two O–H bonds contributed by two corresponding water molecules.

Because the Na^+-OAc^- Coulombic attraction is weakened by the excess electron, the addition of the first water molecule to NaOAc^- is able to break one of the Na–O bonds. For the most stable isomers of neutral $\text{NaOAc}(\text{H}_2\text{O})_n$ clusters, no Na–O bond is broken by the first water molecule; instead, two water molecules are needed to break a Na–O bond. It is easier for the $\text{NaOAc}(\text{H}_2\text{O})_n^-$ anions to form SSIP structures than their neutral counterparts. The SSIP structures of $\text{NaOAc}(\text{H}_2\text{O})_n^-$ anions start to show up at $n = 2$ and become nearly degenerate in energy with the CIP structures at $n = 5$. The SSIP structures for the neutral $\text{NaOAc}(\text{H}_2\text{O})_n$ clusters show up at $n = 6$ and become dominant at $n = 7$. It is worth mentioning that the Na atom prefers to be tetra-coordinated in both anionic and neutral $\text{NaOAc}(\text{H}_2\text{O})_n$ clusters with $n > 3$. For the CIP structures of anionic and neutral $\text{NaOAc}(\text{H}_2\text{O})_n$ with $n > 3$, the Na atom interacts directly with three water molecules and one O atom of the OAc group, except for the bidentate structure in which the Na atom interacts with two water molecules and two O atoms of the OAc group. For the SSIP structures, the Na atom interacts directly with four water molecules.

VI. CONCLUSIONS

We investigated the $\text{NaOAc}(\text{H}_2\text{O})_n^-$ ($n = 0-3$) cluster anions with mass spectrometry and photoelectron spectroscopy. We also conducted quantum chemistry calculations to explore the structures of $\text{NaOAc}(\text{H}_2\text{O})_n^-$ anions and $\text{NaOAc}(\text{H}_2\text{O})_n$ neutrals. Our calculations show that the anionic and neutral $\text{NaOAc}(\text{H}_2\text{O})_n$ clusters have many low-lying isomers. The VDEs of the most stable structures of $\text{NaOAc}(\text{H}_2\text{O})_n^-$ ($n = 0-3$) obtained by theoretical calculations are in agreement with the experimental values. The water molecules can interact with the sodium atom through their O atoms and interact with the oxygen atoms of acetate by forming hydrogen bonds, and thus insert between the Na–O bonds of sodium acetate to form six-membered ring structures. Because the Na^+-OAc^- Coulombic attraction is weakened by the excess electron, it is easier to break the Na–O bonds of NaOAc^- than those of NaOAc. The SSIP structures of $\text{NaOAc}(\text{H}_2\text{O})_n^-$ anions start to show up at $n = 2$ and become nearly degenerate in energy with the CIP structures at $n = 5$; while the SSIP structures for the neutral $\text{NaOAc}(\text{H}_2\text{O})_n$ clusters show up at $n = 6$ and become dominant at $n = 7$.

ACKNOWLEDGMENTS

This work was supported by the National Natural Science Foundation of China (Grant Nos. 21403249 to G.F. and 21273246 to W.J.Z.). The theoretical calculations were

conducted on the ScGrid and DeepComp 7000 of the Supercomputing Center, Computer Network Information Center of Chinese Academy of Sciences.

- ¹A. Kumar and S. S. Pawar, *Tetrahedron* **59**, 5019 (2003).
- ²E. Pines, D. Huppert, and N. Agmon, *J. Phys. Chem.* **95**, 666 (1991).
- ³P. Arosio, B. Jaquet, H. Wu, and M. Morbidelli, *Biophys. Chem.* **168-169**, 19 (2012).
- ⁴D. L. Beauchamp and M. Khajehpour, *Biophys. Chem.* **161**, 29 (2012).
- ⁵F. J. Millero, R. Feistel, D. G. Wright, and T. J. McDougall, *Deep Sea Res., Part I* **55**, 50 (2008).
- ⁶L. Jaeglé, P. K. Quinn, T. S. Bates, B. Alexander, and J. T. Lin, *Atmos. Chem. Phys.* **11**, 3137 (2011).
- ⁷D. Brownstein, *Salt: Your Way to Health* (Medical Alternatives Press, 2006).
- ⁸D. E. Woon and T. H. Dunning, *J. Am. Chem. Soc.* **117**, 1090 (1995).
- ⁹G. H. Peslherbe, B. M. Ladanyi, and J. T. Hynes, *J. Phys. Chem. A* **102**, 4100 (1998).
- ¹⁰C. P. Petersen and M. S. Gordon, *J. Phys. Chem. A* **103**, 4162 (1999).
- ¹¹G. H. Peslherbe, B. M. Ladanyi, and J. T. Hynes, *J. Phys. Chem. A* **104**, 4533 (2000).
- ¹²G. H. Peslherbe, B. M. Ladanyi, and J. T. Hynes, *Chem. Phys.* **258**, 201 (2000).
- ¹³P. Jungwirth, *J. Phys. Chem. A* **104**, 145 (2000).
- ¹⁴S. Yamabe, H. Kouno, and K. Matsumura, *J. Phys. Chem. B* **104**, 10242 (2000).
- ¹⁵P. Jungwirth and D. J. Tobias, *J. Phys. Chem. B* **105**, 10468 (2001).
- ¹⁶S. Godinho, P. C. do Couto, and B. J. C. Cabral, *Chem. Phys. Lett.* **419**, 340 (2006).
- ¹⁷A. C. Olleta, H. M. Lee, and K. S. Kim, *J. Chem. Phys.* **126**, 144311 (2007).
- ¹⁸G. Sciaini, R. Fernandez-Prini, D. A. Estrin, and E. Marceca, *J. Chem. Phys.* **126**, 174504 (2007).
- ¹⁹T. Jin, B. Zhang, J. Song, L. Jiang, Y. Qiu, and W. Zhuang, *J. Phys. Chem. A* **118**, 9157 (2014).
- ²⁰B. S. Ault, *J. Am. Chem. Soc.* **100**, 2426 (1978).
- ²¹G. Gregoire, M. Mons, C. Dedonder-Lardeux, and C. Jouvet, *Eur. Phys. J. D* **1**, 5 (1998).
- ²²G. Gregoire, M. Mons, I. Dimicoli, C. Dedonder-Lardeux, C. Jouvet, S. Martrenchard, and D. Solgadi, *J. Chem. Phys.* **112**, 8794 (2000).
- ²³X. B. Wang, C. F. Ding, J. B. Nicholas, D. A. Dixon, and L. S. Wang, *J. Phys. Chem. A* **103**, 3423 (1999).
- ²⁴C. Dedonder-Lardeux, G. Gregoire, C. Jouvet, S. Martrenchard, and D. Solgadi, *Chem. Rev.* **100**, 4023 (2000).
- ²⁵J. J. Max and C. Chapados, *J. Chem. Phys.* **115**, 2664 (2001).
- ²⁶Q. Zhang, C. J. Carpenter, P. R. Kemper, and M. T. Bowers, *J. Am. Chem. Soc.* **125**, 3341 (2003).
- ²⁷A. Mizoguchi, Y. Ohshima, and Y. Endo, *J. Am. Chem. Soc.* **125**, 1716 (2003).
- ²⁸A. T. Blades, M. Peschke, U. H. Verkerk, and P. Kebarle, *J. Am. Chem. Soc.* **126**, 11995 (2004).
- ²⁹L. Jiang, T. Wende, R. Bergmann, G. Meijer, and K. R. Asmis, *J. Am. Chem. Soc.* **132**, 7398 (2010).
- ³⁰C.-W. Liu, F. Wang, L. Yang, X.-Z. Li, W.-J. Zheng, and Y. Q. Gao, *J. Phys. Chem. B* **118**, 743 (2014).
- ³¹D. J. Tobias and J. C. Hemminger, *Science* **319**, 1197 (2008).
- ³²W. J. Xie and Y. Q. Gao, *J. Phys. Chem. Lett.* **4**, 4247 (2013).
- ³³Y. Feng, M. Cheng, X.-Y. Kong, H.-G. Xu, and W.-J. Zheng, *Phys. Chem. Chem. Phys.* **13**, 15865 (2011).
- ³⁴Z. Zeng, G.-L. Hou, J. Song, G. Feng, H.-G. Xu, and W.-J. Zheng, *Phys. Chem. Chem. Phys.* **17**, 9135 (2015).
- ³⁵R.-Z. Li, C.-W. Liu, Y. Q. Gao, H. Jiang, H.-G. Xu, and W.-J. Zheng, *J. Am. Chem. Soc.* **135**, 5190 (2013).
- ³⁶C.-W. Liu, G.-L. Hou, W.-J. Zheng, and Y. Q. Gao, *Theor. Chem. Acc.* **133**, 1550 (2014).
- ³⁷G. Feng, G.-L. Hou, H.-G. Xu, Z. Zeng, and W.-J. Zheng, *Phys. Chem. Chem. Phys.* **17**, 5624 (2015).
- ³⁸Y. Wang, G. Zhuang, S. Chen, Z. An, and A. Zheng, *Atmos. Res.* **84**, 169 (2007).
- ³⁹Y. L. Zhang, X. Q. Lee, and F. Cao, *Atmos. Environ.* **45**, 413 (2011).
- ⁴⁰B. Ouyang and B. J. Howard, *Phys. Chem. Chem. Phys.* **11**, 366 (2009).
- ⁴¹K. Haupa, A. Bil, A. Barnes, and Z. Mielke, *J. Phys. Chem. A* **119**, 2522 (2015).
- ⁴²H. M. A. Rahman, G. Hefter, and R. Buchner, *J. Phys. Chem. B* **116**, 314 (2012).

- ⁴³X.-B. Wang, B. Jagoda-Cwiklik, C. Chi, X.-P. Xing, M. Zhou, P. Jungwirth, and L.-S. Wang, *Chem. Phys. Lett.* **477**, 41 (2009).
- ⁴⁴K. D. Collins, G. W. Neilson, and J. E. Enderby, *Biophys. Chem.* **128**, 95 (2007).
- ⁴⁵L. Vrbka, J. Vondrasek, B. Jagoda-Cwiklik, R. Vacha, and P. Jungwirth, *Proc. Natl. Acad. Sci. U. S. A.* **103**, 15440 (2006).
- ⁴⁶J. S. Uejio, C. P. Schwartz, A. M. Duffin, W. S. Drisdell, R. C. Cohen, and R. J. Saykally, *Proc. Natl. Acad. Sci. U. S. A.* **105**, 6809 (2008).
- ⁴⁷E. F. Aziz, N. Ottosson, S. Eisebitt, W. Eberhardt, B. Jagoda-Cwiklik, R. Vacha, P. Jungwirth, and B. Winter, *J. Phys. Chem. B* **112**, 12567 (2008).
- ⁴⁸M. Pastorcak, S. T. van der Post, and H. J. Bakker, *Phys. Chem. Chem. Phys.* **15**, 17767 (2013).
- ⁴⁹L.-Y. Wang, Y.-H. Zhang, and L.-J. Zhao, *J. Phys. Chem. A* **109**, 609 (2005).
- ⁵⁰B. Hess and N. F. A. van der Vegt, *Proc. Natl. Acad. Sci. U. S. A.* **106**, 13296 (2009).
- ⁵¹B. Minofar, P. Jungwirth, M. R. Das, W. Kunz, and S. Mahiuddin, *J. Phys. Chem. C* **111**, 8242 (2007).
- ⁵²H. V. R. Annapureddy and L. X. Dang, *J. Phys. Chem. B* **116**, 7492 (2012).
- ⁵³H.-G. Xu, Z.-G. Zhang, Y. Feng, J. Y. Yuan, Y. C. Zhao, and W. J. Zheng, *Chem. Phys. Lett.* **487**, 204 (2010).
- ⁵⁴M. J. Frisch, G. W. Trucks, H. B. Schlegel, G. E. Scuseria, M. A. Robb, J. R. Cheeseman, G. Scalmani, V. Barone, B. Mennucci, G. A. Petersson, H. Nakatsuji, M. Caricato, X. Li, H. P. Hratchian, A. F. Izmaylov, J. Bloino, G. Zheng, J. L. Sonnenberg, M. Hada, M. Ehara, K. Toyota, R. Fukuda, J. Hasegawa, M. Ishida, T. Nakajima, Y. Honda, O. Kitao, H. Nakai, T. Vreven, J. A. Montgomery, Jr., J. E. Peralta, F. Ogliaro, M. Bearpark, J. J. Heyd, E. Brothers, K. N. Kudin, V. N. Staroverov, R. Kobayashi, J. Normand, K. Raghavachari, A. Rendell, J. C. Burant, S. S. Iyengar, J. Tomasi, M. Cossi, N. Rega, J. M. Millam, M. Klene, J. E. Knox, J. B. Cross, V. Bakken, C. Adamo, J. Jaramillo, R. Gomperts, R. E. Stratmann, O. Yazyev, A. J. Austin, R. Cammi, C. Pomelli, J. W. Ochterski, R. L. Martin, K. Morokuma, V. G. Zakrzewski, G. A. Voth, P. Salvador, J. J. Dannenberg, S. Dapprich, A. D. Daniels, O. Farkas, J. B. Foresman, J. V. Ortiz, J. Cioslowski, and D. J. Fox, *GAUSSIAN 09*, Revision A.02, Gaussian, Inc., Wallingford, CT, 2009.
- ⁵⁵Y. Tawada, T. Tsuneda, S. Yanagisawa, T. Yanai, and K. Hirao, *J. Chem. Phys.* **120**, 8425 (2004).
- ⁵⁶O. A. Vydrov, J. Heyd, A. V. Krukau, and G. E. Scuseria, *J. Chem. Phys.* **125**, 074106 (2006).
- ⁵⁷O. A. Vydrov and G. E. Scuseria, *J. Chem. Phys.* **125**, 234109 (2006).
- ⁵⁸O. A. Vydrov, G. E. Scuseria, and J. P. Perdew, *J. Chem. Phys.* **126**, 154109 (2007).
- ⁵⁹J. A. Pople, M. Head-Gordon, and K. Raghavachari, *J. Chem. Phys.* **87**, 5968 (1987).
- ⁶⁰See supplementary material at <http://dx.doi.org/10.1063/1.4927668> for the vibrational progression of NaOAc and the natural bond orbital (NBO) charge distributions of NaOAc⁻ anion and neutral NaOAc.